Korean J. Chem. Eng., 40(4), 714-721 (2023)
DOI: 10.1007/s11814-023-1353-y
pISSN: 0256-1115
eISSN: 1975-7220

REVIEW PAPER

Thermal regeneration characteristics of titanium isopropoxide-modified TiO_2 for the removal of environmentally hazardous NO_x in iron ore sintering process

Yoo-jin Jung*,‡, Beom-Sik Kim,‡, Bora Jeong***, Hong-Dae Kim***, Jong Min Won****, Kwangseo Cha****, and Jin-Sun Cha*,†**

*Material Technology Center, Korea Testing Laboratory, Seoul 08389, Korea
**Department of Chemical and Biomolecular Engineering, Korea Advanced Institute of Science and Technology, Daejeon 34131, Korea
***Green Materials & Processes R&D Group, Ulsan Regional Division, Korea Institute of Industrial Technology, Ulsan 44413, Korea
****R&D Division, Hyundai Steel, Dangjin 31719, Korea
(*Received 25 January 2023 • Revised 16 February 2023 • Accepted 18 February 2023*)

Abstract−The deactivation and thermal regeneration characteristics of a V_2O_5-WO_3/TiO_2 catalyst modified with titanium isopropoxide (TTIP) were investigated after it was applied for 2,400 h at 240 °C in a selective catalytic reduction (SCR) pilot plant to purify the exhaust gas from an iron ore sintering process in steelworks. Evolved gas analysis/mass spectrometry (EGA/MS) analysis was adopted to determine the temperature for thermal regeneration, and thermal treatment was performed at the determined temperature for 3 h in a N_2 atmosphere. The catalysts (Fresh catalyst: N-Cat, used catalyst: U-Cat, and thermally regenerated catalyst: R-Cat-X (X is thermal regeneration temperature)) were analyzed by elemental analyzer, X-ray fluorescence (XRF, component analysis), Brunauer-Emmett-Teller (BET, specific surface area and porosity), scanning electron microscopy-energy dispersive X-ray spectroscopy (SEM-EDS, surface micro-structure and components), X-ray diffraction (XRD, crystalline structure), and Fourier-transform infrared (FT-IR, surface functional group). Thermal regeneration of catalyst was evaluated by NO_x removal efficiency, depending on the regeneration temperature. It was found that the deactivation of the catalyst occurred due to the reduction of specific surface area and porosity by ammonium (bi)sulfate (AS or ABS). The NO_x removal efficiency of the R-Cat-400 and the R-Cat-500 reached to 98.5% and 99.1%, respectively. Due to the breakdown of AS and ABS during the thermal regeneration, those results were quite similar to those of the N-Cat. Although the NO_x removal efficiency of the R-Cat-500 was higher than that of the R-Cat-400, the temperature for thermal regeneration needs to be determined under consideration of the emission of high concentration of SO_2 emitted during thermal regeneration.

Keywords: Selective Catalytic Reduction (SCR), Titanium Oxide, Titanium Isopropoxide (TTIP), Thermal Regeneration, Ammonium (Bi)Sulfate

INTRODUCTION

Urban environmental pollution brought on by municipal solid waste, particulate matter, volatile organic compounds (VOCs), NO_x, SO_x, and global warming is a severe issue worldwide [1-5]. As a solution to urban environmental pollution, bio-oil synthesis through biomass pyrolysis [6-10], bio-hydrogen production via biomass gasification [11-18], bio-diesel synthesis through esterification [19,20], biofuel production [21-23], carbon sequestration using bio-char [24], hydrogen production via water splitting [25-27], and treatment of waste plastics [28-30] can be considered.

Fine dust (PM2.5) has been one of the major air pollution problems in Korea for the past several decades. According to the PM 2.5 measurement results of 35 countries of the Organization for Economic Cooperation and Development (OECD) announced in 2017, the worldwide average PM 2.5 concentration was 12.5 μg/m^3, while Korea had the highest value of 25.1 μg/m^3 [31].

According to the "Comprehensive Measures for Fine Dust Management" jointly announced in 2017, fine dust emissions can be divided into direct emissions and indirect emissions (secondary generation). Although fine dust can be removed by using cyclone or filter [32], indirect emissions refer to the conversion of sulfur oxides (SO_x), nitrogen oxides (NO_x), and volatile organic compounds (VOCs) into fine dust through chemical reactions [33]. In the case of Korea, indirect emissions accounted for 72% of the total emissions nationwide [34]. The "Comprehensive Fine Dust Management Plan", released in 2019, enhanced the emission standards for dust, NO_x, SO_x, ammonia, and hydrogen sulfide, which are the causes of fine dust, to an average of 30% in accordance with the severity of domestic fine dust. In particular, it was announced that air pollution fees for nitrogen oxides will be implemented [35].

NO_x is not only a precursor of fine dust, but also a substance that has harmful effects on the human body and the environment by acting on acid rain, greenhouse gases, ozone depletion, and photochemical smog [36,37]. Various technologies have been developed to remove NO_x, but the selective catalytic reduction (SCR) process, which reduces NO_x to N_2 and H_2O by reacting with the reducing

†To whom correspondence should be addressed.
E-mail: jscha@ktl.re.kr
‡These authors contributed equally.

agent NH_3 on a catalyst, is the most widely used where a large amount of NO_x is generated [38-43]. The most commercially available SCR catalyst is V_2O_5-WO_3 (MoO_3)/TiO_2, which has been widely applied to fossil fuel power plants because of its high activity in the temperature range of 300-400 °C, N_2 selectivity, and resistance to SO_2 [44-46]. However, there is a limit to the application of the catalyst because it is known that gases released from non-electric sectors, such as steel and cement, have different characteristics from those of fossil fuel power plants, such as temperature and exhaust gas composition [47,48].

The steel industry is one of the major domestic emitters of fine dust, accounting for roughly 40% of total fine dust emissions [49]. Recently, as emission standards have been strengthened, the application of the SCR process to steel mills and sintering furnaces has expanded. The SCR of the sintering furnace at the steelworks is a tail-end system installed after the particulate matter removal device and the desulfurization facility. The concentration of SO_2 and particulate matter in the exhaust gas is low, but there is a difficulty in maintaining performance at low temperatures (about 80 to 200 °C) [50]. At that temperature, the commercial catalyst of V_2O_5-WO_3 (MoO_3)/TiO_2 has very low activity, so additional energy must be input to maintain the reaction temperature at around 280 °C [45, 51]. To solve these problems, the need to develop a low-temperature SCR catalyst is emerging, but the poisoning problem of the catalyst is the biggest obstacle to commercializing the low-temperature SCR catalyst [37,47]. In particular, when SO_2 is included in the exhaust gas, SO_2 itself is adsorbed on the catalytic material and is poisoned. At low temperatures below 250 °C, SO_2 and H_2O in the exhaust gas react with the reducing agent NH_3 to produce NH_4HSO_4 (ammonium bisulfate, ABS) or $(NH_4)_2S_2O_7$ (ammonium sulfate, AS) [52,53]. These substances are reported to reduce the activity of the catalyst by blocking the pores of the catalyst or combining with the active site [51]. Since ABS generally decomposes at 350 °C or higher, it has been reported that in-situ regeneration by thermally treating the poisoned catalyst at 350 °C is possible [45]. However, it is reported that the exact decomposition temperature of ABS is affected by the chemical composition of the catalyst [54], and thus it is necessary to set the regeneration temperature through the evaluation of catalyst characteristics.

In this study, a catalyst containing V_2O_5-WO_3 on TiO_2 modified with titanium isopropoxide (TTIP) was prepared and applied to the steel mill sintering process. Although many studies related to developing Ce, Mn, and Cu-based SCR catalysts have been conducted, their resistances to sulfur and water poisoning still require improvement [55-59]. The V_2O_5-WO_3/TiO_2 composition used in this study was selected because it is known to show good sulfur- and water-tolerance. Modification with TTIP was also chosen as a method to improve the low-temperature activity of the catalyst. Lee et al. studied the SCR reaction of a vanadium-based catalyst prepared by modifying TiO_2 as a support with TTIP [60]. The NO_x removal performance at 240 °C increased by more than 10% at most due to the change of the support, which also enlarged the catalyst's active site and improved the dispersity of the active material. Also, it was reported that the resistance to H_2O and SO_2 in the exhaust gas was improved with TTIP compared to the previous catalyst. Therefore, in this study, a honeycomb-type V_2O_5-WO_3/TTIP-modified TiO_2 catalyst was prepared and applied for 2,400 hours at 240 °C in the SCR process at the rear end of the steelworks sintering furnace. The poisoned catalyst was carefully characterized to reveal the main cause of the catalyst degradation during the long-term SCR. Furthermore, *in-situ* thermal regeneration methods for a commercial application were evaluated by analyzing the thermal decomposition behaviors of the catalyst.

EXPERIMENTAL PROCEDURE

1. Catalyst Preparation

The SCR catalyst for steel mill sintering furnace application was manufactured by extrusion molding in the form of honeycomb based on the V_2O_5-WO_3/TiO_2 composition. Ammonium vanadate (AMV, NANO Co.) and ammonium metatungstate (AMT, NANO Co.), which are catalytic components, were dissolved in monoethanolamine (MEA, NANO Co.) and distilled water, and sufficiently ionized. A catalyst composite was prepared by adding it to a solution of titanium (IV) isopropoxide (TTIP, Alfa Aesar) separately dispersed in distilled water, followed by additional stirring. Then, TiO_2 (NANO Co.), organic/inorganic binders, and surfactants were placed into an open kneader. After moderately evaporating moisture in an open kneader at 80 °C, the clay was mixed at 60 °C for 8 h, and vacuum treatment was performed to minimize pores inside the clay. The vacuum-treated clay was extruded in a honeycomb form using a vacuum extrusion molding machine, maintained at room temperature for 24 hours, and then dried in a constant temperature and humidity chamber at 80 °C for 24 hours. A honeycomb type V_2O_5-WO_3/TTIP modified TiO_2 catalyst was prepared by calcinating twice at 350-420 °C. This fresh catalyst sample was denoted as N-Cat.

The prepared catalyst was installed in the SCR pilot plant where the exhaust gas from the sintering furnace of the steel mill was introduced and applied at 240 °C for 2,400 h. The space velocity applied to the site was 4,444 h^{-1}, and the exhaust gas composition of the site is shown in Table 1. After the experiment, the catalyst applied to the sintering furnace of the steel mill was denoted as U-Cat.

2. Thermal Regeneration

The decomposition temperature of catalyst poisoning components was analyzed by evolved gas analysis/mass spectrometry (EGA/MS). For analysis, a pyrolyzer (EGA/Py-3030D, Frontier Lab.) connected to GC/MS (7890A/5975, Agilent) was used. After 10 mg of the catalyst was loaded into the pyrolyzer, it was heated from 100 °C to 800 °C at a rate of 20 °C/min, and the gas generated as the temperature increased was analyzed with a mass spectrometer. The components of the generated gas were analyzed by referring to the National Institute of Standards and Technology (NIST) library 08. After the thermal regeneration temperature was selected based on the results of EGA/MS, N_2 gas was flowed at a face velocity of 10 m/h, and thermal regeneration was performed for three hours at

Table 1. Composition of exhaust gas emitted from the sintering process

Gas composition	NO_x	SO_x	CO	CO_2	H_2O	O_2
Concentration	150-220	30-50	1%	5%	10%	15%

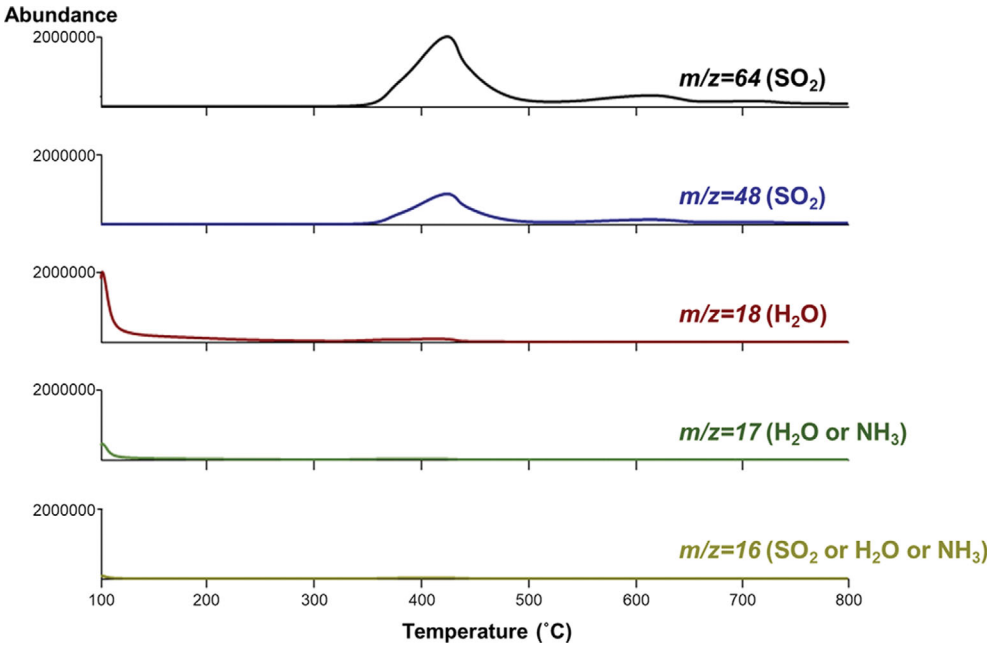

Fig. 1. Results of evolved gas analysis/mass spectrometry (EGA/MS) analysis for the U-Cat.

each temperature. The thermally regenerated catalyst was denoted as R-Cat-X, and X represents the thermal regeneration temperature.

3. Catalytic Activity Measurement

The performance of the catalyst was measured in a micro reactor by applying the round-robin test conditions of the VGB Guideline. The gas composition for catalytic performance evaluation before and after application to steelworks was NO_x 300 ppm, SO_2 300 ppm, NH_3 300 ppm, O_2 5%, and H_2O 10%. When evaluating the NO_x removal efficiency, an area velocity of 10 m/h and a temperature of 240 °C were applied. The gas concentration after the reaction was analyzed using a NO_x analyzer (T200H, Teledyne), SO_2 analyzer (T100H, Teledyne), O_2 analyzer (OXITEC-5000, ENOTECH), and NH_3 analyzer (Airwell+7, KINSCO). The NO_x removal efficiency was calculated by applying the formula below:

$$NO_x \text{ removal efficiency } (\%) = \frac{NO_x^{in} - NO_x^{out}}{NO_x^{in}} \times 100$$

4. Catalyst Characterization

To evaluate the characteristics of each catalyst, elemental analysis, component analysis, specific surface area and pore characteristics, micro-surface shape and components, and surface functional groups were analyzed. Using an elemental analyzer, elements including C, H, N, and S were examined to learn more about the elemental characteristics of the catalyst (2400 Series II, PerkinElmer). The chemical composition was analyzed by X-ray fluorescence (XRF), ZSX Primus IV, Rigaku. The specific surface area and pore characteristics of the catalyst were analyzed using N_2 adsorption-desorption (3 Flex, Micromeritics) after pretreatment in a vacuum atmosphere at 150 °C. Microsurface morphology and components were analyzed with scanning electron microscopy (SEM, MIRA 3 XMU, TESCAN) and energy dispersive X-ray spectrometer (EDS, X-act, OXFORD) equipment connected to SEM. The change in crystal phase structure of the catalyst was analyzed by X-ray diffraction (XRD, X'pert PRO, Panalytical). The XRD analysis was performed under Cu Kα radiation, 2θ=10-90° conditions. Surface functional groups were analyzed by FT-IR (VERTEX 70, Bruker) after preparing a disk form by mixing pulverized catalyst powder with KBr. Wavenumber range at this time was analyzed under 4,000-400 cm^{-1} with 4 cm^{-1} resolution.

RESULTS AND DISCUSSION

1. Thermal Regeneration

The components of the gas created by the catalyst were tested according to temperature using EGA/MS, and the findings are given in Fig. 1 in order to calculate the thermal regeneration temperature of the catalyst used in the sintering furnace in steelworks. For SO_2, m/z=64 and 48, for H_2O, m/z=18, and for H_2O or NH_3, m/z=17. The results showed that H_2O and NH_3 decomposed at a low temperature of less than 200 °C, whereas SO_2 started decomposition at about 350 °C and formed the highest peak at 425 °C. This SO_2 evolution peak implied the desorption of adsorbed SO_2 or decomposition of ammonium (bi)sulfates (ABS). Based on these EGA/MS results, the catalysts applied to the steelworks sintering furnace were thermally regenerated at 300, 400, and 500 °C for three hours, respectively, and then the deNO_x performance and characteristic changes were examined.

2. Catalytic Performance

Fig. 2 shows the NO_x removal performance of the catalyst before and after application to the steel mill sintering furnace and the regenerated catalyst by thermal regeneration temperature. The deNO_x efficiency of the N-Cat was 93.8%, but the performance of the catalyst after 2,400 hours of application in the steelworks was about 65%, which was analyzed to reduce the efficiency by about 30.7% compared to the new catalyst. For the effect of the thermal regeneration temperature, the deNO_x efficiency of the catalyst thermally

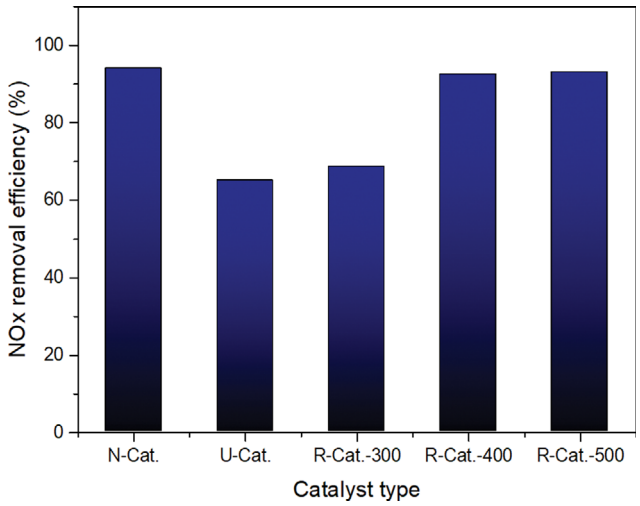

Fig. 2. NO_x removal efficiency of the catalysts.

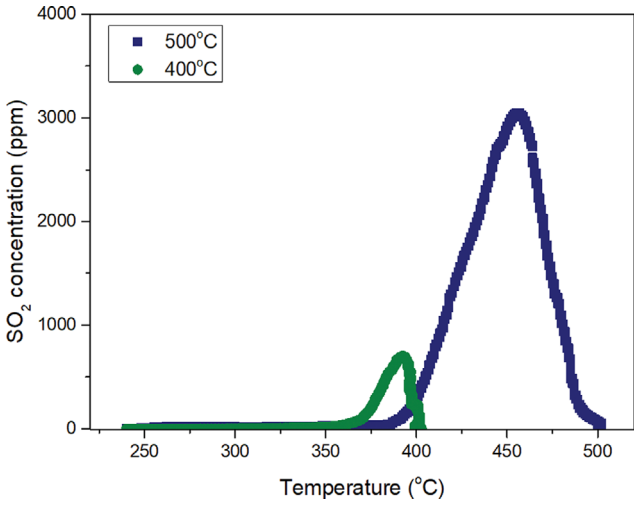

Fig. 3. SO_2 emission concentration by the thermal regeneration temperature.

regenerated at 300 °C was 68.5%, showing little improvement in efficiency after thermal regeneration. On the other hand, as the thermal regeneration temperature increased, the deNO_x efficiency of the catalyst increased to 92.4% in the R-Cat-400 and 93.0% in the R-Cat-500, and it was evaluated that the performance was restored to a performance similar to that of the fresh catalyst. A number of studies on the regeneration of SCR catalysts applied to coal- or biomass-fired power plants have been reported [36,61,62]. According to these reports, the catalysts were poisoned by various materials, such as alkali and alkaline earth metals (Ca, Na, and K), heavy metals (As and Pb), Cl, and P, as well as AS/ABS. Off-site regeneration methods, such as solution washing, have been widely used to regenerate the poisoned catalysts. However, these methods require additional process and significant operating cost. Recently, in order to solve this problem, *in-situ* regeneration methods using high-temperature steam were applied and reported [63]. It is well known that high-temperature steam regeneration can effectively remove water-soluble elements like K, As, Fe, Ca, and Na in addition to sulfate species. As shown in Fig. 2, the thermal regeneration was able to fully restore the catalytic performance of the V_2O_5-WO_3/TTIP-modified TiO_2 catalyst that had been harmed by the exhaust from the sintering of iron ore.

Fig. 3 shows the result of measuring the concentration of SO_2 emitted during thermal regeneration. At 400 °C thermal regeneration, the maximum SO_2 concentration was about 700 ppm, while at 500 °C it was analyzed to be about 3,000 ppm, indicating that the SO_2 emission concentration increased as the thermal regeneration temperature increased. According to this result, ABS decomposition and SO_2 desorption were facilitated when the thermal regeneration temperature was increased to 500 °C. Although a larger amount of SO_2 could be emitted during thermal regeneration at

Table 2. Elemental and chemical composition of the catalysts

	Element	N-Cat	U-Cat	R-Cat-300	R-Cat-400	R-Cat-500
Elemental composition (wt%)	C	0.03	0.04	0.02	0.03	0.00
	H	0.25	0.70	0.42	0.26	0.22
	N	0.06	0.30	0.25	0.08	0.04
	S	0.32	1.85	1.77	1.02	0.23
Chemical composition (wt%)	TiO_2	79.9	76.3	75.6	77.2	79.4
	V_2O_5	4.58	4.14	4.33	4.48	4.45
	WO_3	2.12	1.87	1.92	1.98	2.05
	SiO_2	7.28	7.52	7.73	7.63	7.41
	Al_2O_3	2.28	2.22	2.30	2.30	2.21
	CaO	1.69	1.75	1.72	1.71	1.69
	Na_2O	0.062	0.085	0.116	0.101	0.099
	MgO	0.258	0.267	0.265	0.257	0.259
	P_2O_5	0.052	0.078	0.082	0.084	0.085
	SO_3	0.816	5.13	5.13	3.46	1.33
	K_2O	0.105	0.101	0.109	0.109	0.114
	Fe_2O_3	0.359	0.360	0.372	0.387	0.399

Table 3. Specific surface area and porosity of the catalysts

	N-Cat	U-Cat	R-Cat-300	R-Cat-400	R-Cat-500
BET surface area (m^2/g)	55	52	52	54	57
Total pore volume (cm^3/g)	0.25	0.23	0.24	0.25	0.26
Average pore diameter (nm)	18.2	17.9	18.4	18.5	18.4

Table 4. Surface chemical composition of the catalysts analyzed by XRF

	Element	N-Cat	U-Cat	R-Cat-300	R-Cat-400	R-Cat-500
Chemical composition (wt%)	C	3.73	3.71	3.88	3.99	4.63
	O	48.68	50.02	48.37	47.13	48.18
	Si	1.59	1.90	1.50	1.33	1.60
	S	0.32	1.95	1.98	0.95	0.46
	Ti	43.00	39.54	41.75	44.39	42.77
	V	2.68	2.25	2.52	2.20	2.35

500 °C, there is no significant difference in the NO_x removal performance between the R-Cat-400 and R-Cat-500 catalysts (Fig. 2). Therefore, it should be taken into account that selecting a suitable regeneration temperature is vital in terms of energy usage and environmental impact.

3. Catalyst Surface Characteristics

Table 2 shows the results of elemental analysis and chemical composition analysis of the catalyst before and after application to the steelworks sintering furnace and the regeneration catalyst by thermal regeneration temperature. For the U-Cat applied to the steelworks sintering furnace for 2,400 hours, it was analyzed that the concentrations of N and S increased significantly compared to the new catalyst, and the concentration of H also increased, suggesting that poisoning by substances containing N, S, and H occurred. R-Cat-500 demonstrated outcomes comparable to those of the fresh catalyst (N-Cat) as the element concentration gradually decreased as the thermal regeneration temperature increased.

XRF analysis showed that there was no change in the main components of the catalyst (TiO_2, V_2O_5, and WO_3) after application to the steelworks sintering furnace exhaust, and the poisoning effect by alkali and alkaline earth metal substances, such as Na, K, Ca, and Mg, was not insignificant. Since the sintering exhaust did not contain alkali/alkaline earth metals, it was apparent that the poisoned SCR catalyst could be sufficiently regenerated by thermal regeneration only. However, elemental analysis revealed that the SO_3 content increased by over six times, indicating that poisoning by sulfur-containing compounds did indeed occur. In terms of the effect of thermal regeneration temperature, the $S(SO_3)$ concentration in the R-Cat-300 was nearly identical to that of the U-Cat, so thermal regeneration at the corresponding temperature had no significant effect on the decrease in S concentration. On the other hand, as the thermal regeneration temperature increased, the $S(SO_3)$ content in the catalyst tended to decrease.

Table 3 shows the specific surface area and pore characteristics. It was analyzed that the specific surface area, total pore volume, and average pore size of the catalyst were slightly reduced compared to the N-Cat. Shi et al. explained that the total pore volume of a catalyst is related to the specific surface area, and that the reduction in the total pore volume of the catalyst used is due to clogging of some pores, which also reduces the specific surface area [64]. Thus, it is determined that the specific surface area and pore volume are reduced due to the clogging of the pores of the catalyst by the poisoning substance.

For the specific surface area and pore characteristics of the catalyst for each thermal regeneration temperature, recovery of the specific surface area was hardly observed in the R-Cat-300. On the other hand, when the thermal regeneration temperature increased to 400 °C, the specific surface area increased to 98.7% compared to the new catalyst, and when increased to 500 °C, the specific surface area and pore characteristics were recovered to the level of the fresh catalyst.

Fig. 4 summarizes the SEM and EDS mapping results for each catalyst type, and Table 4 displays the EDS measurement results. The temperature of the SCR applied to the steelworks' sintering furnace was 240 °C, which was not a high operating temperature, and thus it was found that there was no significant change in the catalyst surface itself. In the XRD analysis of Fig. 6, the main crystal structure was determined to be TiO_2 anatase (2θ=25.3, 37.8, 48.0, 53.9, 55.10) [65,66], and it was believed that there was no change in the crystal structure.

As a result of the EDS measurement in Table 4, the S content increased significantly after the application of the steelworks sintering furnace, and the distribution map by mapping also showed that the S distribution on the catalyst surface increased, indicating that poisoning by S-containing materials occurred. Looking at the results according to the thermal regeneration temperature, the S content gradually decreased as the thermal regeneration temperature increased, in the same manner as the elemental analysis and XRF results, and the distribution of S on the catalyst surface also decreased in the mapping result. Thus, it is clear that when the thermal regeneration temperature rose, the rate of disintegration and removal of the S-containing substance poisoning the catalyst surface increased.

Fig. 5 shows the results of crystal phase analysis by catalyst type. It was analyzed that TiO_2 anatase was maintained in the crystal phase structure of the catalyst even after thermal regeneration. This led

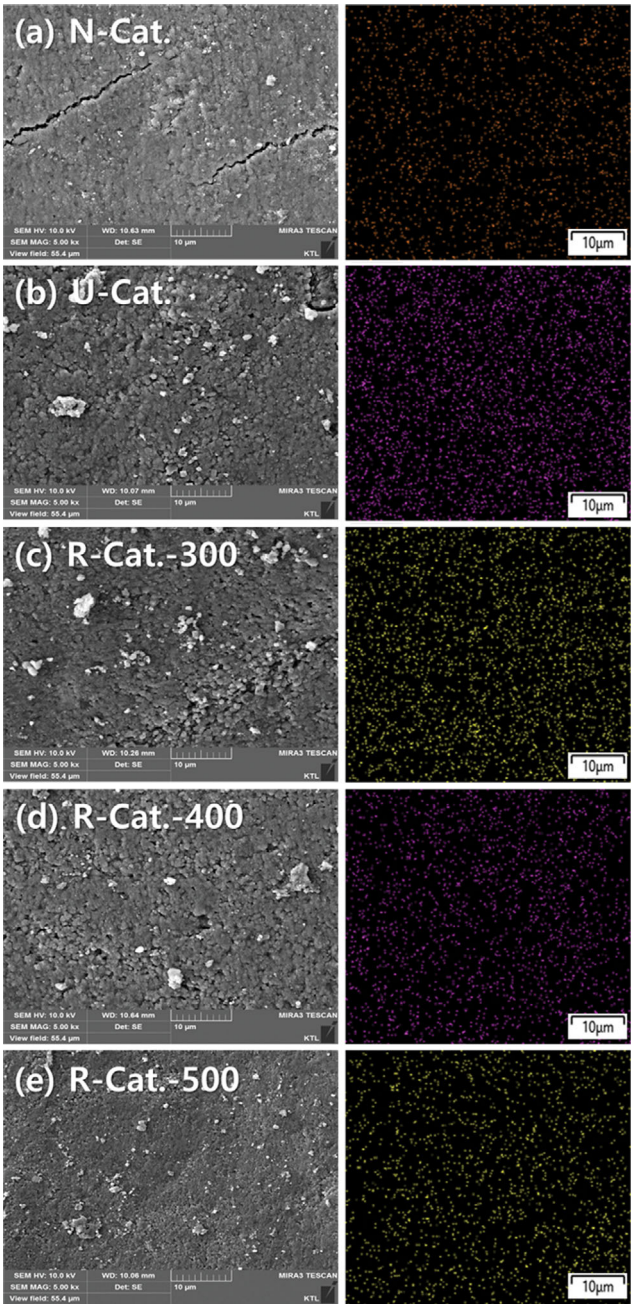

Fig. 4. Scanning electron microscopy (SEM) image and energy dispersive X-ray spectroscopy (EDS) mapping results of (a) N-Cat, (b) U-Cat, (c) R-Cat-300, (d) R-Cat-400, and (e) R-Cat-500.

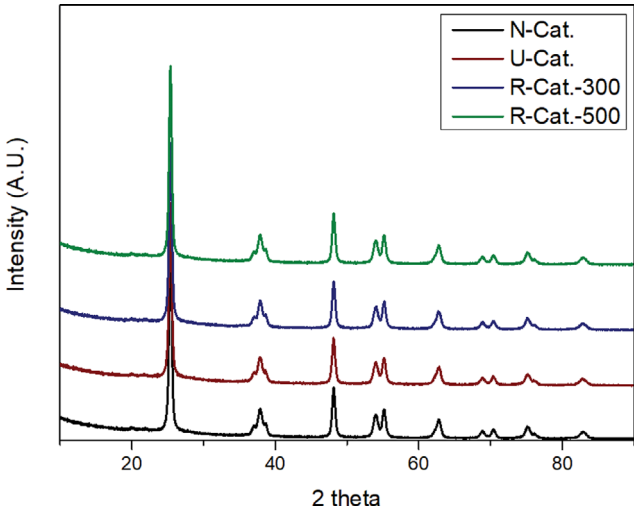

Fig. 5. X-ray diffraction (XRD) patterns of the catalysts.

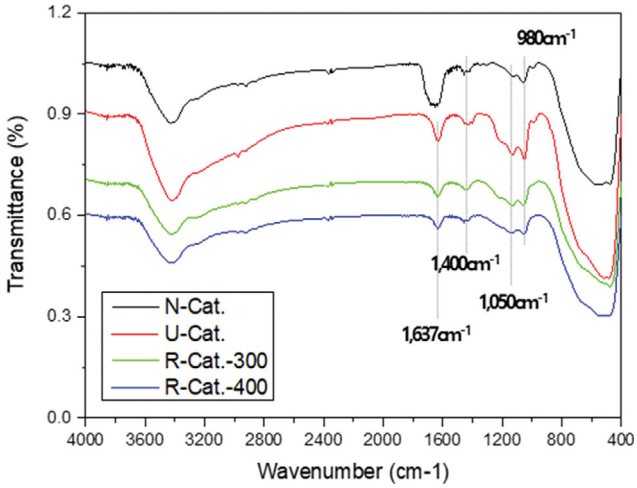

Fig. 6. Fourier transform-infrared (FT-IR) spectra of the catalysts.

to the conclusion that the catalyst renewal process can be carried out at temperatures of up to 500 °C.

Fig. 6 shows the FT-IR analysis results for each type of catalyst. After applying the steel mill sintering furnace, it was found that the FT-IR peaks increased at about 980 cm^{-1}, 1,050 cm^{-1}, and 1,400 cm^{-1}. These findings are consistent with those in earlier works, and Cimino et al. explained that 1,050 cm^{-1} is the result of TiO_2 sulfation [67]. In addition, it was explained that the 1,400 cm^{-1} band detected in the sulfated V_2O_5/TiO_2 catalyst was caused by the asymmetric bending vibration of NH_4^+. Guo et al. reported that the formation of $SO_4^{2-}NH_4^+$ bands on the catalyst surface after the SO_2 resistance reaction was caused by ammonium (bi)sulfate deposition on the catalyst surface [47]. Through the previous elemental and component analysis results, it was believed that the activity of the catalyst was reduced by ammonium (bi)sulfate deposition formed on the catalyst applied to the steelworks sintering furnace as the N, H, and S content increased.

In addition, peaks such as 1,050 cm^{-1} and 1,400 cm^{-1} decreased as the thermal regeneration temperature increased, and in Fig. 2, the NO_x removal efficiency recovered to the level of the new catalyst at a thermal regeneration temperature of 400 °C or higher. Wang et al. explained that when the poisoned V/W/Ti catalyst was thermally regenerated at 400 °C, the SCR catalyst activity was improved to the level of a new catalyst because the main reason for the deactivation of the catalyst was the formation of ammonium bisulfate or ammonium sulfate [68,69]. Specifically, it was hypothesized in this work that As and ABS, which contaminated the catalyst by thermal regeneration, were broken down, allowing the

catalytic performance to be recovered.

CONCLUSION

A sulfur- and water-tolerant V_2O_5-WO_3/TiO_2-based SCR catalyst was prepared by modification with titanium isopropoxide (TTIP). This catalyst was applied to the removal of NO_x in iron ore sintering process exhaust and its long-term degradation characteristics was investigated. Thermal regeneration behavior was also examined to consider *in-situ* regeneration of catalyst. It was found that the main cause of the performance degradation of TTIP-modified TiO_2 catalyst was the decrease of surface area and pore volume resulting from the formation of ammonium (bi)sulfates (AS and ABS), which are poisonous substances. As the thermal regeneration temperature increased from 300 to 500 °C, the removal rate of the AS and ABS was improved, and the recovery rate of the specific surface area and pore characteristics of the catalyst also increased accordingly. As a result, compared to the fresh catalyst, the catalyst performance improved by 98.5% for R-Cat-400 and 99.1% for R-Cat-500, respectively. It is believed that the problem of exceeding the acceptable emission concentration may arise when applied to the industrial field because when the thermal regeneration temperature grows, the concentration of SO_2 produced by the breakdown of AS and ABS increases. Examining long-term thermal regeneration experiments at a temperature where SO_2 starts to be decomposed and released for each catalyst is important to control large concentrations of SO_2 from being emitted. Therefore, considering those points, future studies should focus on the recovery of the performance of the sulfur-poisoned catalyst with regeneration temperature and time.

ACKNOWLEDGEMENT

This work was supported by the Korea Ministry of Trade, Industry and Energy (MOTIE) as "Development of NO_x Removal Catalyst with Wide Temperature Window (No. 20005721)".

REFERENCES

1. J.-R. Youn, M.-J. Kim, S.-J. Lee, I.-S. Ryu, S. K. Jeong, K. Lee and S. G. Jeon, *Korean J. Chem. Eng.*, **39**, 2334 (2022).
2. O. A. Qamar, F. Jamil, M. Hussain, A. H. Al-Muhtaseb, A. Inayat, A. Waris, P. Akhter and Y.-K. Park, *Chem. Eng. J.*, **454**, 140240 (2023).
3. J. E. Lee, Y. S. Ok, D. C. W. Tsang, J. H. Song, S.-C. Jung and Y.-K. Park, *Sci. Total Environ.*, **719**, 137405 (2020).
4. U. Asghar, S. Rafiq, A. Anwar, T. Iqbal, A. Ahmed, F. Jamil, M. S. Khurram, M. M. Akbar, A. Farooq, N. S. Shah and Y.-K. Park, *J. Environ. Chem. Eng.*, **9**(5), 106064 (2021).
5. J. Lee, W.-H. Chen and Y.-K. Park, *Bioresour. Technol.*, **366**, 128204 (2022).
6. M. W. Seo, S. H. Lee, H. Nam, D. Lee, D. Tokmurzin, S. Wang and Y.-K. Park, *Bioresour. Technol.*, **343**, 126109 (2022).
7. H. W. Ryu, D. H. Kim, J. Jae, S. S. Lam, E. D. Park and Y.-K. Park, *Bioresour. Technol.*, **310**, 123473 (2020).
8. J.-Y. Kim, H. W. Lee, S. M. Lee, J. Jae and Y.-K. Park, *Bioresour. Technol.*, **279**, 373 (2019).
9. S. Oh, J. Lee, S. S. Lam, E. E. Kwon, J.-M. Ha, D. C. W. Tsang, Y. S. Ok, W.-H. Chen and Y.-K. Park, *Bioresour. Technol.*, **342**, 126067 (2021).
10. S. Valizadeh, S. Pyo, Y.-M. Kim, H. Hakimian and Y.-K. Park, *Chem. Eng. J.*, **450**, 137971 (2022).
11. D. Lee, H. Nam, M. W. Seo, S. H Lee, D. Tokmurzin, S. Wang and Y.-K. Park, *Chem. Eng. J.*, **447**, 137501 (2022).
12. S. Moogi, S. S. Lam, W.-H. Chen, C. H. Ko, S.-C. Jung and Y.-K. Park, *Bioresour. Technol.*, **366**, 128209 (2022).
13. S. Valizadeh, H. Hakimian, A. Farooq, B.-H. Jeon, W.-H. Chen, S. H. Lee, S.-C. Jung, M. W. Seo and Y.-K. Park, *Bioresour. Technol.*, **365**, 128143 (2022).
14. S. Valizadeh, S.-H. Jang, G. H. Rhee, J. Lee, P. L. Show, M. A. Khan, B.-H. Jeon, K.-Y. A. Lin, C. H. Ko, W.-H. Chen and Y.-K. Park, *Chem. Eng. J.*, **433**, 133793 (2022).
15. S. Valizadeh, Y. Khani, A. Farooq, G. Kumar, P. L. Show, W.-H. Chen, S. H. Lee and Y.-K. Park, *Bioresour. Technol.*, **372**, 128638 (2023).
16. H. Yim, S. Valizadeh, S. Pyo, S.-H. Jang, C. H. Ko, M. A. Khan, B.-H. Jeon, K.-Y. A. Lin and Y.-K. Park, *Fuel*, **338**, 127243 (2023).
17. S. Valizadeh, Y. Khani, H. Yim, S. Chai, D. Chang, A. Farooq, P.-L. Show, B.-H. Jeon, M. A. Khan, S.-C. Jung and Y.-K. Park, *Environ. Res.*, **219**, 115070 (2023).
18. J. Seo, H. Kim, S. Jeon, S. Valizadeh, Y. Khani, B.-H. Jeon, G. H. Rhee, W.-H. Chen, S. S. Lam, M. A. Khan and Y.-K. Park, *Bioresour. Technol.*, **373**, 128702 (2023).
19. U. Shakeel, M. Hussain, R. Sheikh, A. Ahmed, M. S. Nazir, W. Yang, N. Shezad, P. Akhter and Y.-K. Park, *Korean J. Chem. Eng.*, **38**, 966 (2021).
20. I. Riaz, I. Shafiq, F. Jamil, A. H. Al-Muhtaseb, P. Akhter, S. Shafique, Y.-K. Park and M. Hussain, *Catal. Rev.*, in press (DOI: 10.1080/01614940.2022.2108197) (2022).
21. S. Nawaz, F. Jamil, P. Akhter, M. Hussain, H. Jang and Y.-K. Park, *J. Phys. Energy*, **5**, 012003 (2023).
22. H. P. R. Kannapu, S. Pyo, S. S. Lam, J. Jae, G. H. Rhee, M. A. Khan, B.-H. Jeon and Y.-K. Park, *Bioresour. Technol.*, **359**, 127500 (2022).
23. A. Farooq, S. S. Lam, G. H. Rhee, J. Lee, M. A. Khan, B.-H. Jeon and Y.-K. Park, *Bioresour. Technol.*, **353**, 127131 (2022).
24. J. Y. Seo, D. Tokmurzin, D. Lee, S. H. Lee, M. W. Seo and Y.-K. Park, *Bioresour. Technol.*, **361**, 127740 (2022).
25. P. Bhavani, D. P. Kumar, M. Hussain, K.-J. Jeon and Y.-K. Park, *Catal. Rev.*, in press (DOI: 10.1080/01614940.2022.2038472) (2022).
26. P. Bhavani, D. P. Kumar, M. Hussain, T. M. Aminabhavi and Y.-K. Park, *Chem. Eng. J.*, **434**, 134743 (2022).
27. J. E. Lee, K.-J. Jeon, P. L. Show, I. H. Lee, S.-C. Jung, Y. J. Choi, G. H. Rhee, K.-Y. A. Lin and Y.-K. Park, *Fuel*, **308**, 122048 (2022).
28. S. Lee, J. Lee and Y.-K. Park, *ACS Sustainable Chem. Eng.*, **10**(42), 13972 (2022).
29. J. Lee, E. E. Kwon, S. S. Lam, W.-H. Chen, J. Rinklebe and Y.-K. Park, *J. Clean. Prod.*, **321**, 128989 (2021).
30. Y.-K. Park and J. Lee, *Phytochem. Rev.*, in press (DOI: 10.1007/s11101-021-09788-8) (2022).
31. H.-S. Kim, S. Kasipandi, J. Kim, S.-H. Kang, J.-H. Kim, J.-H. Ryu and J.-W. Bae, *Catalysts*, **10**, 52 (2020).
32. J.-S. Youn, S. Han, J.-S. Yi, D.-I. Kang, K.-W. Jang, Y.-W. Jung, Y.-K.

Park and K.-J. Jeon, *Environ. Res.*, **193**, 110507 (2021).
33. Y.-K. Park, W. G. Shim, S.-C. Jung, H.-Y. Jung and S. C. Kim, *Korean J. Chem. Eng.*, **39**, 161 (2022).
34. The Government of the Republic of Korea, *Comprehensive Plan on Fine dust Management* (2017).
35. The Government of the Republic of Korea, *Comprehensive Plan on Fine dust Management* (2019).
36. S. Zhao, J. Peng, R. Ge, K. Yang, S. Wu, Y. Qian, T. e Xu, J. Gao, Y. Chen and Z. Sun, *Process Saf. Environ. Prot.*, **168**, 971 (2022).
37. Z. Liu, J. Han, L. Zhao, Y.-w. Wu, H.-x. Wang, X.-q. Pei, M.-x, Xu, Q. Lu and Y.-p. Yang, *Appl. Catal. A: Gen.*, **587**, 117263 (2019).
38. Y.-k. Yu, C. He, J.-s. Chen and X.-r. Meng, *J. Fuel Chem. Tech.*, **40**, 1359 (2012).
39. S. Fu, G. Cao, G. Ou, F. Zhou and L. Li, *Korean J. Chem. Eng.*, **39**, 1717 (2022).
40. W. Jin, C. Geng, Y. Wang, H. Ma, Y. Dong and F. Si, *Korean J. Chem. Eng.*, **38**, 771 (2021).
41. F. Gao, X. Jin, G. Wang, L. Sun, Y. Tan, R. Zhang, W. Zhao, J. Hou and R. Zhang, *Environ. Eng. Res.*, **28**(1), 210500 (2023).
42. L. Zhao, Y. Zhang and M. Kang, *Environ. Eng. Res.*, **27**(1), 200642 (2022).
43. Y.-J. Jung, J.-S. Cha, S.-J. Lim, J.-W. Park, M.-C. Shin and Y.-K. Park, *Energy Environ.*, 0958305X221101152 (2022).
44. X. Zhang, Q. Diao, X. Hu, X. Wu, K. Xiao and J. Wang, *Nanomaterials*, **10**, 1900 (2020).
45. L. Song, J. Chao, Y. Fang, H. He, J. Li, W. Qiu and G. Zhang, *Chem. Eng. J.*, **303**, 275 (2016).
46. S. T. Choo, S. D. Yim, I.-S. Nam, S.-W. Ham and J.-B. Lee, *Appl. Catal. B: Environ.*, **44**(3), 237 (2003).
47. K. Guo, J. Ji, W. Song, J. Sun, C. Tang and L. Dong, *Appl. Catal. B: Environ.*, **297**, 120388 (2021).
48. T. Lee and H. Bai, *AIMS Environ. Sci.*, **3**(2), 261 (2016).
49. C. H. Lee, J. H. Choi, M. S. Kim, B. H. Seo, C. H. Kang and D.-H. Lim, *Clean Technol.*, **27**(4), 332 (2021).
50. H. Zhu, L. Song, K. Li, R. Wu, W. Qiu and H. He, *Catalysts*, **12**, 341 (2022).
51. X. Guo, C. Bartholomew, W. Hecker and L. L. Baxter, *Appl. Catal. B: Environ.*, **92**(1-2), 30 (2009).
52. L. Xu, C. Wang, H. Chang, Q. Wu, T. Zhang and J. Li, *Environ. Sci. Tech.*, **52**(12), 7064 (2018).
53. P. Li, Q. Liu and Z. Liu, *Chem. Eng. J.*, **181-182**, 169 (2012).
54. Z. Zhu, H. Niu, Z. Liu and S. Liu, *J. Catal.*, **195**(2), 268 (2000).
55. C. Tang, H. Zhang and L. Dong, *Catal. Sci. Tech.*, **6**, 1248 (2016).
56. L.-g. Wei, R.-t. Guo, J. Zhou, B. Qin, X. Chen, Z.-x. Bi and W.-g. Pan, *Fuel*, **316**, 123438 (2022).
57. Y. Peng, W. Jiang, Y. Liu, L. Yao, Y. Chen and L. Yang, *J. Environ. Chem. Eng.*, **10**, 108799 (2022).
58. D. Damma, P. R. Ettireddy, B. M. Reddy and P. G. Smioniotis, *Catalysts*, **9**(4), 349 (2019).
59. G. Xu, X. Guo, X. Cheng, J. Yu and B. Fang, *Nanoscale*, **13**(15), 7052 (2021).
60. G. Lee, B. Ye, M.-j. Lee, S.-Y. Chun, B. Jeong, H.-D. Km, J. Jae and T. Kim, *J. Ind. Eng. Chem.*, **109**, 422 (2022).
61. X. Shang, G. Hu, C. He, J. Zhao, F. Zhang, Y. Xu, Y. Zhang, J. Li and J. Chen, *Ind. Eng. Chem.*, **18**, 513 (2012).
62. S. Zhao, J. Peng, R. Ge, K. Yang, S. Wu, Y. Qian, T. Xu, J. Gao, Y. Chen and Z. Sun, *Process Saf. Environ.*, **168**, 971 (2022).
63. H. Pan, E.-h. Gao, T.-t. Fang, Y. Mei, Y. He and Y. Shi, *Appl. Surf. Sci.*, **541**, 148408 (2021).
64. Y. Shi, P. Zhang, T. Fang, E. Gao, F. Xi, T. Shou, M. Tao, S. Wu, M. T. Bernards, Y. He and H. Pan, *Catal. Comm.*, **116**, 57 (2018).
65. N. Zhao, S. Pan and Z. Wei, *Adv. Mat. Res.*, **807-809**, 1431 (2013).
66. L. Zong, F. Dong, G. Zhang, W. Han, Z. Tang and J. Zhang, *Catal. Surv. Asia*, **21**, 103 (2017).
67. S. Cimino, C. Ferone, R. Cio, G. Perillo and L. Lisi, *Catalysts*, **9**, 464 (2019).
68. Y. Wang, W. Yi, J. Yu, J. Zeng and H. Chang, *Environ. Sci. Tech.*, **54**, 12612 (2020).
69. X. Wang, X. Du, L. Zhang, Y. Chen, G. Yang and J. Ran, *Appl. Catal. A: Gen.*, **559**, 112 (2018).